PROCEEDINGS OF SCIENCE

Measurement of the ^{30}S+α system for type I X-ray bursts

D. Kahl[*a], **A. A. Chen**[b], **S. Kubono**[a], **T. Hashimoto**[a], **D. N. Binh**[a], **J. Chen**[b], **S. Cherubini**[c], **N. N. Duy**[d], **S. Hayakawa**[a], **N. Iwasa**[e], **H. S. Jung**[f], **S. Kato**[g], **Y. K. Kwon**[f], **S. Michimasa**[a], **S. Nishimura**[h], **S. Ota**[a], **K. Setoodehnia**[b], **T. Teranishi**[i], **H. Tokieda**[a], **T. Yamada**[e], **H. Yamaguchi**[a], **C. C. Yun**[f], **L. Y. Zhang**[j]
[a] *Center for Nuclear Study, the University of Tokyo, Japan*
[b] *Department of Physics & Astronomy, McMaster University, Canada*
[c] *Department of Physics, University of Catania & INFN-LNS, Italy*
[d] *Institute of Physics, Vietnam Academy of Science and Technology, Vietnam*
[e] *Department of Physics, Tohoku University, Japan*
[f] *Department of Physics, Chung-Ang University, Korea*
[g] *Depatment of Physics, Yamagata University, Japan*
[h] *RIKEN (The Institute of Physical and Chemical Research), Japan*
[i] *Department of Physics, Kyushu University, Japan*
[j] *Institute of Modern Physics, Chinese Academy of Sciences, China*
E-mail: `daid@cns.s.u-tokyo.ac.jp`

The ^{30}S(α, p) reaction is considered to be important in the nuclear trajectory to higher mass in type I X-ray bursts. The reaction flow encounters a bottle-neck at ^{30}S, owing to the competition of photo-disintegration with further proton capture, and because the half-life of this isotope is on the order of the burst rise timescale. Different burst simulations by various researchers indicate the (α, p) reaction may by-pass this waiting point, depending on the stellar reaction rate, which has not previously been measured experimentally, and the structure of the compound nucleus ^{34}Ar is not well understood above the alpha-threshold. The ^{30}S(α, p) reaction could explain rare bolometrically double-peaked burst profiles, appears to make a considerable contribution to the overall energy generation, and affects the neutron star crustal composition for the recurrent inertia required in burst models to reproduce astronomical observations. Using a low-energy ^{30}S radioactive ion beam and an active target technique (a helium gas mixture serves as both a target gas and a detector fill gas), we acquired data on both alpha elastic scattering of ^{30}S as well as the ^{30}S(α, p) reaction simultaneously at relevant energies for X-ray bursts. We present for the first time the status of the data analysis and the preliminary results of this research.

XII International Symposium on Nuclei in the Cosmos
August 5-12, 2012
Cairns, Australia

---

[*] Speaker.

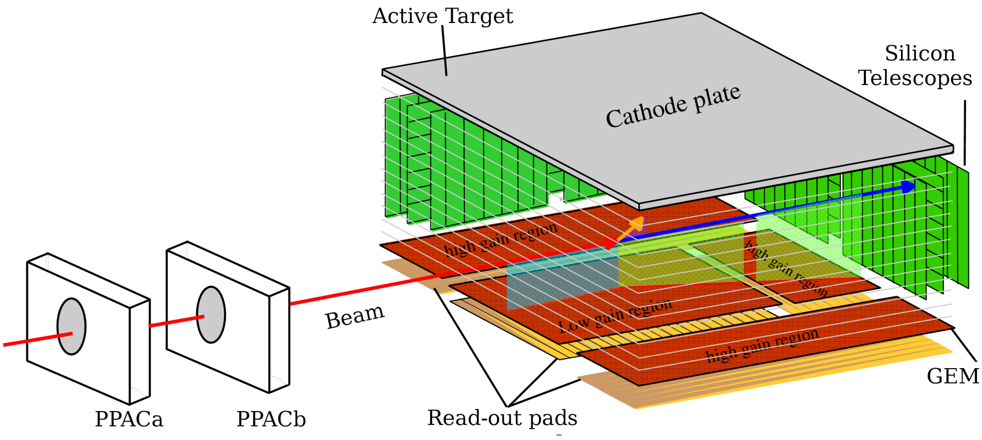

Figure 1: Schematic of experimental setup, consisting of two PPACs, the active target, and silicon telescope arrays. Note that between PPACb and the active target, the beam impinges on a kapton foil (7.5 μm), which retains the active target fill gas. The beam is tracked in the central low gain region ("active target region," 19 cm), surrounded on three sides by high gain GEMs and silicon telescopes to measure outgoing light ions (right side telescope not depicted). Beneath each GEM is a readout pattern, separated into 4 mm thick backgammon pads. ΔE is simply proportional to the collected charge of each pad. The coordinate system is one where the beam axis defines positive Z, the rest following standard right-handed conventions. Z and X positions are determined by the pad number and comparing charge collection on either side of the backgammon, respectively. The Y position is determined by the electron drift time.

1. Introduction

Type I X-ray bursts result from thermonuclear runaway in the hydrogen- and helium-rich accreted envelopes on neutron stars in close binary systems [1]. As the bursts are not powerful enough to disrupt the binary star system, they recur typically on the order of hours or days, making them the most frequent thermonuclear explosions in the galaxy. While the nuclear reaction network involves several hundred nuclear species linked by a few thousand nuclear processes, certain reactions are of particular interest; one such reaction is the ^{30}S(α, p) reaction.

The ^{30}S(α,p) reaction rate is important to the overall energy generation of X-ray bursts [2], influences the neutron star crustal composition [3], and may explain the bolometric double-peaked nature of some rare X-ray bursts [4]. Very recent studies are finally exploring the excited states of the compound nucleus ^{34}Ar well above the alpha-threshold to experimentally constrain this reaction rate [5, 6]; unfortunately, any important states must have energies near $E_x \simeq 9.0 \pm 1.2$ MeV (corresponding to the peak burst temperature of 1.3 GK) with a large Γ_α, which cannot be inferred from these works. Here we report the analysis status of the first-ever measurement of the ^{30}S+α system, performed at the astrophysically relevant energies with an active target and an RI beam.

2. Method

The measurement of the ^{30}S + α system was performed at CRIB [7, 8] using the thick target inverse kinematics method [9]. A ^{28}Si^{9+} primary beam was accelerated to 7.32 MeV/u by an

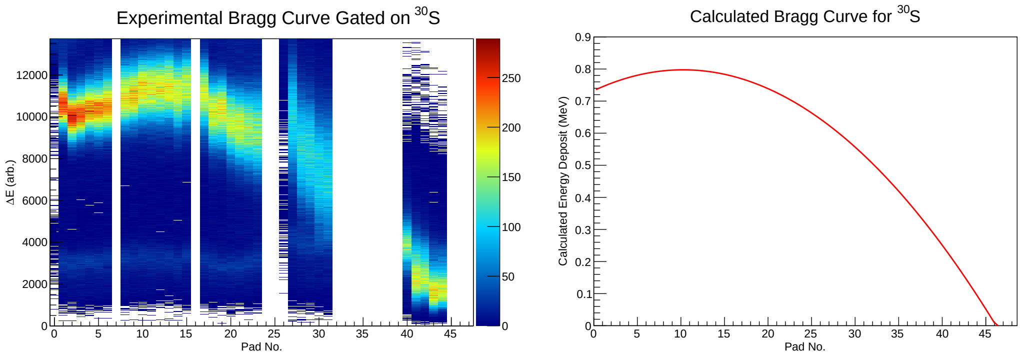

(a) Experimentally measured Bragg curve for ^{30}S.

(b) Calculated Bragg curve for ^{30}S.

Figure 2: Bragg curve for ^{30}S from experiment (a) and calculation (b). The abscissa is target depth (Z), determined by the pad number, where each pad is 4 mm in length. The ordinate is energy deposit. The calculation reasonably reproduces the experimental data. Some data are absent in the experimental histogram from either poor quality or faulty electronics.

AVF cyclotron at RIKEN, arrived at the CRIB entrance focal plane impinging on our cryogenic (90 K) production target [10] filled with ^{3}He gas of thickness 1.68 mg/cm^2 (400 Torr), producing the secondary beam ion of interest via the ^{3}He(^{28}Si ,^{30}S)n reaction. The cocktail beam then passed either a 2.5 μm Be stripper foil or a 220 μg/cm^2 C foil to boost the population of fully-stripped ions, was momentum selected at the dispersive focal plane for ^{30}S^{16+} at 4.0 MeV/u ($\Delta p/p = 1.875\%$), and finally purified with the Wien (velocity) filter (±72 kV) before arriving at the experimental focal plane. The main impurity was ^{29}P^{15+}, which has a production cross section around $\sim 10^2$ mb/sr [11], about two orders of magnitude higher than ^{30}S under these conditions ($\sim$ 1 mb/sr) [12]. Further details on the RI beam production and required development were reported previously [13, 14, 15, 16].

The experimental setup is comprised of beam monitors, an active target, and silicon $\Delta E - E$ telescopes, depicted in Figure 1. The beam monitors are parallel plate avalanche counters (PPACs) [17], serving as part of the DAQ trigger as well as calibration points for the active target. Our recently developed active target, called the GEM-MSTPC, couples gas electron multiplier foils (GEMs) [18] to the previous multi-sampling and tracking proportional chamber design (MSTPC) [19, 20]; this setup allows for a higher beam-injection rate. The active target is so called because the fill gas of 90% He serves simultaneously as a helium target and as an ionization gas for passing radiation (the remaining 10% is CO$_2$ as a quenching gas to inhibit secondary ionization); it is capable of measuring charged particle energy losses and trajectories in three dimensions. The GEM-MSTPC is divided into the central region, which has a lower gain for tracking the beam ions and heavy recoils, surrounded on three sides by high gain regions for tracking lighter ejectiles; the gas-pressure was set to 194 Torr to stop the beam before the high-gain region. $\Delta E - E$ telescopes are set outside the GEM-MSTPC to measure the position and residual energy of light ions. Each telescope consists of three Si layers, each layer being 500 μm thick, 9 × 9 cm^2, with 8 strips on one side. The Si detectors are oriented orthogonally, creating 10 × 10 mm^2 pixels.

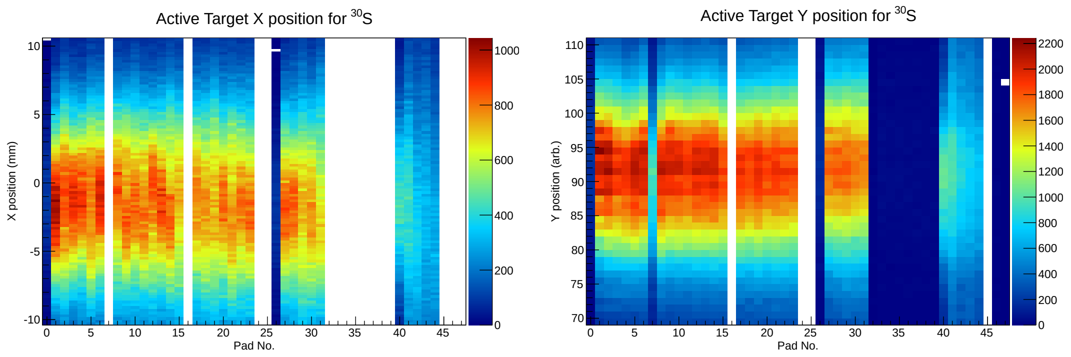

(a) ^{30}S X vs. Z position.

(b) ^{30}S Y vs. Z position.

Figure 3: Measured position of ^{30}S ions within the active target, horizontal (a) and vertical (b) both against target depth (each pad is 4 mm). Horizontal position is determined by comparing the collected charge at the left and right side of the backgammon. Vertical position is determined by electron drift time.

3. Results

Operating with a primary beam intensity of 80 pnA delivered to the CRIB production target, for the three-day data collection run, we achieved an average ^{30}S intensity and purity of $\sim 10^4$ particles per second and 30%, respectively, injected into the active target. The typical energy of the ^{30}S beam at the beginning of the active region was 31.4 MeV, corresponding to $E_{cm} = 3.7$ MeV; the beam is fully stopped by the end of the active region, so that statistics and Rutherford scattering aside, we scan down to $E_{cm} = 0$ MeV. Here we show the analysis of the beam tracking within the GEM-MSTPC, when software gates are placed on ^{30}S ions within the PPACs. Figure 2 shows the experimentally measured Bragg curve of ^{30}S along-side the calculated one; the effective thickness of the detector and target materials was experimentally determined by directly measuring the beam energy at various gas pressures. Figure 3 shows the X and Y positions, respectively, versus Z. Although some detector channels did not function properly, the Bragg curve is well reproduced, and there is no apparent difficulty in tracking the beam in physical space.

In the future, we will extend the analysis to include light ions, in order to reconstruct scattering and reaction kinematics.

References

[1] Wallace, R. K. & Woosley, S. E., *The Astrophysical Journal Supplement* **45** (1981) 389.

[2] Parikh, A., José, J., Moreno, F. & Iliadis, C., *The Astrophysical Journal Supplement* **178** (2008) 110.

[3] Schatz, H. & Rehm, K. E., *Nuclear Physics A* **777** (2006) 601.

[4] Fisker, J. L., Thielemann, F.-K. & Wiescher, M., *The Astrophysical Journal* **608** (2004) L61.

[5] O'Brien, S., Adachi, T., Berg, G. P. A., Couder, M., Dozono, M., Fujita, H., Fujita, Y., Görres, J., Hatanaka, K., Ishikawa, D., Kubo, T., Matsubara, H., Namiki, Y., Ohkuma, Y., Okamura, H., Ong, H. J., Patel, D., Sakemi, Y., Sault, K., Shimbara, Y., Suzuki, S., Suzuki, T., Tamii, A., Wakasa, T., Wantanabe, R., Wiescher, M., Yamada, R. & Zenihiro, J., *American Institute of Physics Conference Series* **1090** (2009) 288.

[6] Deibel, C. M., Rehm, K. E., Figueira, J. M., Greene, J. P., Jiang, C. L., Kay, B. P., Lee, H. Y., Lighthall, J. C., Marley, S. T., Pardo, R. C., Patel, N., Paul, M., Ugalde, C., Woodard, A., Wuosmaa, A. H. & Zinkann, G., *Physical Review C* **84** (2011) 045802.

[7] Kubono, S., Yanagisawa, Y., Teranishi, T., Kato, S., Kishida, Y., Michimasa, S., Ohshiro, Y., Shimoura, S., Ue, K., Watanabe, S. & Yamazaki, N., *European Physical Journal A* **13** (2002) 217.

[8] Yanagisawa, Y., Kubono, S., Teranishi, T., Ue, K., Michimasa, S., Notani, M., He, J. J., Ohshiro, Y., Shimoura, S., Watanabe, S., Yamazaki, N., Iwasaki, H., Kato, S., Kishida, T., Morikawa, T. & Mizoi, Y., *Nuclear Instruments and Methods in Physics Research A* **539** (2005) 74.

[9] Artemov, K. P., Belyanin, O. P., Vetoshkin, A. L., Wolskj, R., Golovkov, M. S., Gol'dberg, V. Z., Madeja, M., Pankratov, V. V., Serikov, I. N., Timofeev, V. A., Shadrin, V. N. & Szmider, J., *Soviet Journal of Nuclear Physics* **52** (1990) 408.

[10] Yamaguchi, H., Wakabayashi, Y., Amadio, G., Hayakawa, S., Fujikawa, H., Kubono, S., He, J. J., Kim, A. & Binh, D. N., *Nuclear Instruments and Methods in Physics Research A* **589** (2008) 150.

[11] Dykoski, W. W. & Dehnhard, D., *Physical Review C* **13** (1976) 80.

[12] Greenfield, M. B., Bingham, C. R., Newman, E. & Saltmarsh, M. J., *Physical Review C* **6** (1972) 1756.

[13] Kahl, D., Chen, A. A., Chen, J., Hayakawa, S., Kim, A., Kubono, S., Michimasa, S., Setoodehnia, K., Wakabayashi, Y. & Yamaguchi, H., *Astronomical Society of the Pacific Conference Series* **393** (2008) 219.

[14] Kahl, D., Chen, A. A., Binh, D. N., Chen, J., Hashimoto, T., Hayakawa, S., Kim, A., Kubono, S., Kurihara, Y., Lee, N. H., Michimasa, S., Nishimura, S., Ouellet, C. V., Setoodehnia, K., Wakabayashi, Y. & Yamaguchi, H., *Proceedings of Science* **NIC X** (2008) 171.

[15] Kahl, D., Chen, A. A., Kubono, S., Binh, D. N., Chen, J., Hashimoto, T., Hayakawa, S., Kaji, D., Kim, A., Kurihara, Y., Lee, N. H., Nishimura, S., Ohshiro, Y., Setoodeh Nia, K., Wakabayashi, Y. & Yamaguchi, H., *American Institute of Physics Conference Series* **1269** (2010) 424.

[16] Kahl, D., Chen, A. A., Kubono, S., Binh, D. N., Chen, J., Hashimoto, T., Hayakawa, S., Kaji, D., Kim, A., Kurihara, Y., Lee, N. H., Ohshiro, Y., Nishimura, S., Setoodeh Nia, K., Wakabayashi, Y. & Yamaguchi, H., *American Institute of Physics Conference Series* **1213** (2010) 208.

[17] Kumagai, H., Ozawa, A., Fukuda, N., Sümmerer, K. & Tanihata, I., *Nuclear Instruments and Methods in Physics Research A* **470** (2001) 562.

[18] Sauli, F., *Nuclear Instruments and Methods in Physics Research A* **386** (1997) 531.

[19] Mizoi, Y., Fukuda, T., Matsuyama, Y., Miyachi, T., Nakano, J., Fukuda, N., Hirai, M., Kobinata, H., Watanabe, Y. X., Sakurai, H., Watanabe, Y. & Yoshida, A., *Nuclear Instruments and Methods in Physics Research A* **431** (1999) 112.

[20] Hashimoto, T., Ishiyama, H., Ishikawa, T., Kawamura, T., Nakai, K., Watanabe, Y. X., Miyatake, H., Tanaka, M. H., Fuchi, Y., Yoshikawa, N., Jeong, S. C., Katayama, I., Nomura, T., Furukawa, T., Mitsuoka, S., Nishio, K., Matsuda, M., Ikezoe, H., Fukuda, T., Das, S. K., Saha, P. K., Mizoi, Y., Komatsubara, T., Yamaguchi, M. & Tagishi, Y., *Nuclear Instruments and Methods in Physics Research A* **556** (2006) 339.